Eurographics Workshop on Visual Computing for Biomedicine (2008)
C. P. Botha, G. Kindlmann, W. J. Niessen, and B. Preim (Editors)

High-Quality Multimodal Volume Visualization of Intracerebral Pathological Tissue

Christian Rieder[†1], Michael Schwier[‡1], Horst K. Hahn[§1] and Heinz-Otto Peitgen[¶1]

[1]MeVis Research GmbH, Center for Medical Image Computing, Bremen, Germany

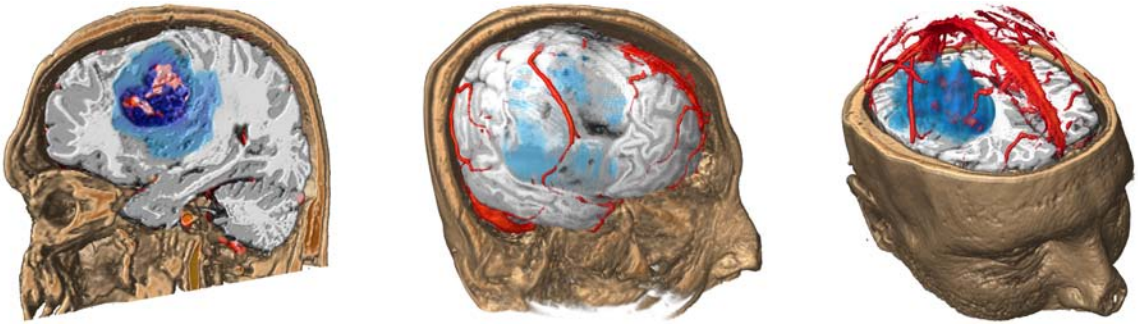

Abstract

Parallel visualization of multiple MRI sequences in 2D is a standard method for exploration of pathological structures for neurosurgery planning. In this work our aim is to support visualization techniques that allow medical experts a fast and comprehensive combined exploration of anatomical structures with inhomogeneous pathological tissue in the three-dimensional volume rendering. The prototypical software solution presented in this paper addresses the issue that a high amount of interaction is commonly needed to merge different MRI sequences and that the resulting visualization does not allow to recognize anatomical details of the brain and pathological tissue at the same time without loss of information. We also present novel clipping methods for neurological volume exploration and emphasize important structures as well as suspicious high intensity signals from multiple sequences in the volume rendering. We demonstrate that our methods facilitate comprehensive volume visualization for neurosurgery.

Categories and Subject Descriptors (according to ACM CCS): J.3 [Life And Medical Sciences]: Health; I.4.10 [Image Presentation]: Volumetric;

1. Introduction

The visualization of intracerebral pathological tissue as well as perifocal edema is an important part of preoperative planning for neurosurgery. However, the pathological information of tumor tissue related to anatomical structures is not sufficiently presented in a single magnetic resonance (MR) data set. In the clinical routine, multispectral image acquisition protocols including different MRI sequences are standard. Common clinical software platforms for neurosurgical planning provide techniques for visualizing multiple MRI sequences in 2D, e.g. merging color coded information of additional data sets. Merging is also possible in the three-dimensional volume rendering where two data sets can be blended using a user specified threshold or alpha blending. Clipping planes can be defined for exploration. The disadvantage of these methods is that the pathological structures

† christian.rieder@mevis.de
‡ michael.schwier@mevis.de
§ horst.hahn@mevis.de
¶ peitgen@mevis.de

as well as risk structures cannot be visualized at the same time with the related anatomy without significant loss of information. Also, substantial interaction is needed to position cutting planes for exploration of tumor tissue and surrounding structures.

The goal of our work is to allow neurosurgeons the three-dimensional volume exploration of diseased intracerebral anatomy combined with information about tumor tissue from multispectral MRI which is not visible in a single data set. In this paper we present advanced blending techniques for the simultaneous high-quality visualization of anatomical structures and intracerebral pathological tissue using multimodal MRI sequences as well as intuitive cutting tools for volume exploration:

- We automatically identify suspicious intensity values from the additional data sets using fuzzy clustering. To blend the high intensity values with the anatomical structures as the white and gray brain matter, we automatically specify a blending transfer function from the analyzed intensity values of the identified structure of interest.
- To suppress unimportant structures, we automatically compute a region of interest (ROI) from a user marked point of interest (POI) using intensity analysis along cast rays in the volume.
- We apply a boundary enhancement algorithm which is based on bump mapping on cutting surfaces to enhance the anatomical boundaries blended with structures from the additional data sets.
- To allow the medical experts a fast and intuitive data observation we introduce the automatic axis aligned cutting tool. We divide the volume into eight octants and hide those octants which are located between view point and ROI.
- We introduce brain peeling as a new method to support intuitive exploration of structures located in the vicinity of the brain surface. Using this technique the surface of the brain can be peeled away step by step in negative normal direction.

2. Related Work

Neuro-visualization is becoming a hot topic in the visualization community. Beyer et al. [BHWB07] present methods for the visualization of multimodal data for neurosurgery planning of deeply seated lesions. In their framework they integrated solutions to simulate skin incisions and removal of the cranial bone as well as brain surface visualization. Different from our solely MRI image based approach they use CT and MRI data sets combined with functional data sets. In [JBB*08] methods for visualization of fMRI data combined with anatomy of the brain are presented. Hong et al. [HBKS05] present compositing functions for multimodal volume fusion. Interactive visualization techniques for combining multimodal data sets are discussed in [BBM*07] to assist neurosurgical planning. Köhn et al. present in [KWK*07] an application for neurosurgical planning and assessing of risk structures. In their work they visualize vessels as well as functional data such as fMRI activation areas and fiber tracts from DTI. Rieder et al. present in [RRRP08] a prototype for visualization of multimodal data for neurosurgical tumor treatment. They describe methods to enhance important functional data and visualize these data combined with anatomical data along a virtual access path.

In few works multi-spectral data of different MRI sequences are used for volume visualization. Kniss et al. [KSW*04] report on a new approach for visualizing multi-field MRI data sets. In [PAG03] a method for the combined visualization of T_1 sequences with *FLAIR* sequences is presented. However, these methods do not allow the visualization of both data sets at the same time without loss of information due to merging.

Bruckner et al. [BGK06] and Viola et al. [VFSG06] propose alternatives to geometric clipping techniques for volume visualization. The developed techniques allow for perceiving context information by exploring the interior of data sets. For neurosurgical data sets interactive clipping tools [WEE03] are a good choice to visualize anatomical details occluded by the brain surface itself. In [SSA*08] the clipping geometry is transformed with respect to the direction of fiber tracts. Tappenbeck et al. [TPD06] introduce slicing equidistant to the lung lobe surface for exploration. Rezk-Salama et al. [RSK06] introduce the opacity peeling algorithm which enables the exploration of the brain surface and clipping of occluding structures without segmentation. Their main idea is to follow the viewing ray through the volume accumulating the opacity until it reaches a threshold. Instead of stopping calculation at this point they reset the accumulation and keep tracing the ray, thus defining several layers which can be removed consecutively to reveal occluded structures. The main drawbacks of this technique are that it is completely view-dependent and that it is sensitive to multiple user-defined parameters. The skull peeling method of Beyer et al. [BHWB07] improved the idea of opacity peeling to overcome those drawbacks and especially meet the requirements of neurosurgical applications. They utilize CT and MRI images to detect the brain surface. The view-dependency is solved by using a depth image. Furthermore they introduce an additional interactive clipping to simulate the skin incision and subsequent bone removal.

3. Preprocessing and Data Analysis

The clinical standard protocol in neurosurgery is to acquire multiple MRI data sets with different sequences. These data sets have to be combined in visualization tools, so that all important features are visible.

In the T_1-*weighted* MRI sequence water results in low signal intensity as well as most lesions and the intensity of fat

tissue is very high. T_1-*weighted* data sets are mostly used for exploration of anatomical structures. The majority of brain tumors are hypointense compared with the brain matter. Additionally, a contrast agent can be injected to intensify the contrast of vessels (T_1ce – *contrast enhancing*). The second often used sequence is the T_2-*weighted* MRI. In this sequence fluids have higher signal intensities than the brain parenchyma and white matter can be very well distinguished from gray matter. An often used advanced T_2-sequence is the *FLAIR* (Fluid Attenuated Inversion Recovery) where the signal of free water is suppressed. In both T_2-sequences pathological tissue is mostly hyperintense compared with the brain parenchyma and can be well distinguished from healthy tissue. However, inhomogeneous lesion tissue can be better recognized with *FLAIR* sequences because of the reduction of the free water signal i.e. in the ventricle and sulca. Figure 1 shows the MRI sequences used in this work.

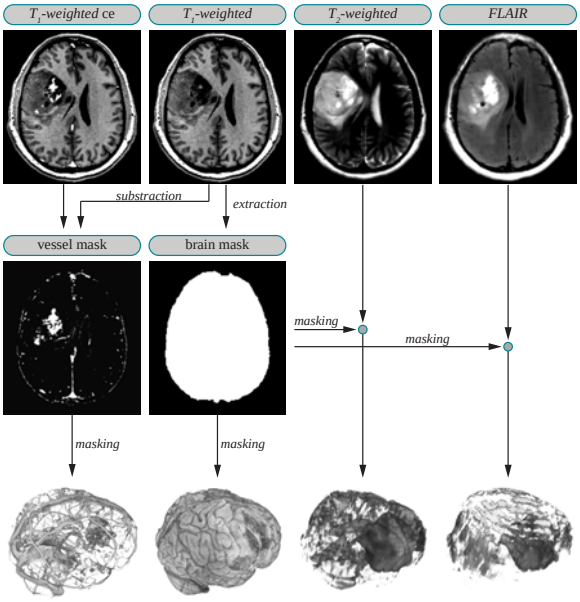

Figure 1: *With the four used MRI sequences and the computed masks, the brain surface, vessels and pathological structures can be visualized.*

To visualize these multiple MRI sequences the data sets have to be registered. The registration is facile to achieve because the patient motion as well as the motion of the brain itself is small and these data sets are acquired in a single MRI session. The registration is done automatically with affine transformations using the entropy-based mutual information [PMV03] as similarity measure. The T_1-*weighted* data set is used as reference for the registration. After preprocessing, the user just has to validate the resulting registration.

To enable the visualization of the brain surface we automatically extract a brain mask using a robust watershed based skull stripping algorithm [HP00]. Since all data sets are registered to the T_1-*weighted* data set, the brain mask can be used with all sequences. Hence, the vessels can be easily extracted using the difference image from the T_1 contrast enhanced data set and the data set without contrast agent. Volume rendering can be used to visualize anatomical details from the MRI sequences combined with a vessel or brain mask. Therefore, a technique for blending additional information from these sequences with anatomical details is required.

To calculate the suspicious high intensity values indicating potential pathological tissue from additional data sets we utilize the fuzzy c-means (FCM) clustering [Bez81] due to its robustness to noise and to varying intensity distributions. The FCM algorithm has already been successfully applied e.g. in MR image segmentation [BHC93] and threshold determination for liver vessel visualization [SDP08]. In order to determine a minimal intensity threshold of the pathological structures two clusters are calculated. The cluster with the higher cluster center – thus the highest mean intensity – now represents the pathologic structures. Subsequently the minimal intensity in this cluster is evaluated and used as an intensity threshold to set up a transfer function for blending. Figure 2 (a) shows the *FLAIR* data set and (b) the resulting clusters computed using fuzzy c-means.

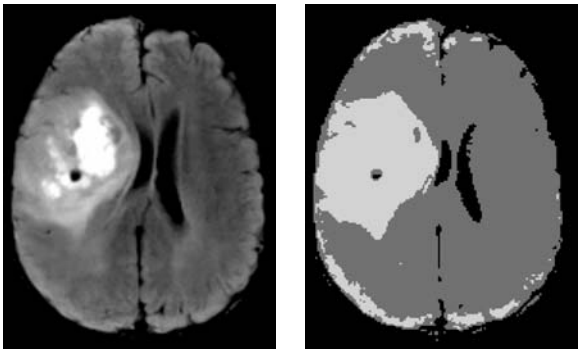

(a) (b)

Figure 2: *Using fuzzy c-means, a FLAIR data set (a) can be divided into $N = 2$ clusters (b). The first cluster contains the lesion as well as the perifocal edema and the second cluster contains the brain matter.*

4. Visualization of Inhomogeneous Pathological Tissue

Visualizing diseased structures is important for exploration of neurological data. Because some tumors cannot be distinguished from healthy structures in T_1-*weighted* images the use of additional sequences such as T_2-*weighted* or *FLAIR* images is standard.

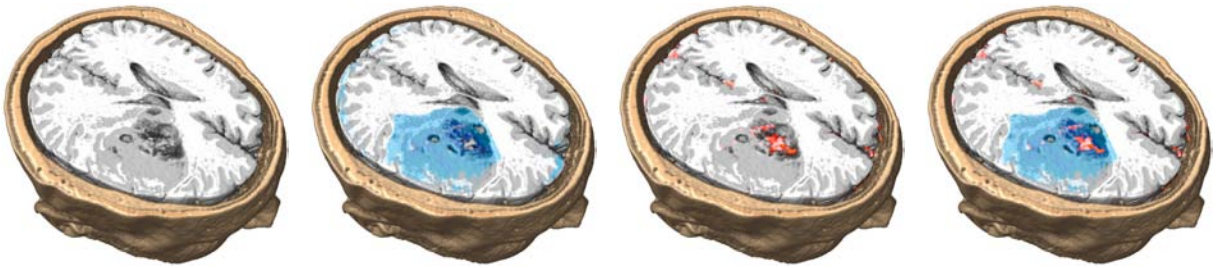

(a) (b) (c) (d)

Figure 3: *Image (a) shows the T_1-weighted data set without blending additional data sets. In (b) the T_1-weighted data set is blended with the FLAIR data set. The high intensity values are color coded blue and include unimportant structures at the brain boundary. Image (c) shows the color coded structures of the vessel mask and (d) the combination of all data sets, the FLAIR data set is blended using the ROI so that unimportant structures are hidden (see also color plate).*

4.1. Visualization of Structures Enhanced with Contrast Agent

The contrast enhanced T_1 data sets show structures like vessels because of the flow of the contrast agent. But additionally there are also other structures visible. If the blood-brain barrier is interrupted near lesions, blood flows into the brain parenchyma and is visible. Thus high activation areas of tumors as well as surrounding tissue are enhanced in the T_1-*weighted ce* sequence. For blending, we compare the voxel of the vessel mask and the corresponding voxel of the T_1 volume to specify which voxel has the higher intensity value. Hence, the voxel with the higher intensity value is rendered so that structures supplied with blood are visible (see Figure 3 (c)).

4.2. Automatic Transfer Function Calculation for Blending of T_2-*weighted* Data

To blend anatomical structures visualized using T_1-*weighted* data sets with pathological structures, e.g. the suspicious high intensity values from a *FLAIR* data set have to be calculated. Just these high intensities are used for blending because most tumors are hyperintense in *FLAIR* images and could be not visible in other data sets. The mean deviation of intensities of unimportant structures like healthy brain matter defines then the minimal intensity threshold because these structures are not needed for blending.

We automatically compute a transfer function for blending using histogram analysis of the fuzzy clustered data set. This transfer function maps the suspicious intensity values of the additional data set to a color gradient (see Figure 3 (b)). The transfer function is set up as a ramp, defined from the intensity threshold to the maximal intensity value of the data set. To blend the color values $\boldsymbol{c}_{FLAIR}$ of the transfer function with the color $\boldsymbol{c}_{T_1}$ of the T_1-*weighted* data set, we calculate the resulting voxel color $\boldsymbol{c}_{rgb\alpha}$ using the following equation:

$$\boldsymbol{c}_{rgb\alpha} = \boldsymbol{c}_{T_1}(1 - a_{mix}) + \boldsymbol{c}_{FLAIR}(a_{mix})$$

where a_{mix} specifies how to mix the data sets, depending on the alpha value α_{FLAIR} of the *FLAIR* data set:

$$a_{mix} = max(1 - (\alpha_{FLAIR} * 0.5), \alpha_{T_1 ce})$$

To get more complex color mappings, the fuzzy cluster can be reclustered with FCM in N clusters, where the mean intensity of each cluster is used to define a support point with color information of the transfer function.

4.3. Attenuation of Unimportant Structures

Some data sets have several structures whose intensity is as high as the intensity of the pathological tissue. In Figure 2 (b) such structures are located at the brain surface. These structures can increase the complexity of the visualization (see Figure 3 (b)). Because of that we integrate a technique which allows the user to attenuate unimportant structures. The user has to mark a point of interest (POI) in the tumor tissue, close to the middle point. From this POI we cast N rays to specify a region of interest (ROI). We achieved good results with $N = 6$ rays. Three rays are cast along the coordinate system axes and three against the direction of the axes to get the intensity of every voxel along those rays. As soon as the intensity becomes less than the intensity threshold the ray got out of the suspicious structure and the distance to the POI is computed. The maximal distance of these six rays is used to specify the spherical ROI. Now only voxels in that ROI are blended with the additional volume (see Figure 3 (d)).

4.4. Boundary Enhancement of Anatomical Structures

The problem of blending color maps with anatomical structures is that important anatomical structures could be attenuated. But the goal is to visualize additional information, e.g. the intensity height of T_2-*weighted* MRT data, with T_1-*weighted* images, so that the underlying anatomical structures are also visible.

Because of that we use additional boundary enhancement on cutting surfaces. To get correct illumination results on cutting planes, on-the-fly gradient computation [HKRs*06] is required. If a planar geometry cuts the volume, all voxels at the edge have the same gradient which is the resulting surface normal. So the illumination of theses voxels is identical. Our idea is to create an effect comparable with bump mapping [Bli78]. In the bump mapping approach, the direction of the surface normal is perturbed to change the illumination. With the locally changed illumination realistic looking surfaces are simulated.

We transformed this idea to volume rendering to enhance anatomical structures, clipped by cutting planes. To manipulate the gradients on the surface we use the intensity values after classification for the gradient computation. Figure 4 illustrates the transformation of the gradients using on-the-fly gradient computation. In this example, the volume has two different intensity values. The gradient direction is manipulated at the boundary of these structures, whereas all other gradients still have the same direction. Consequently the gradients of edge voxels are no more equal and the illumination changes at the boundaries.

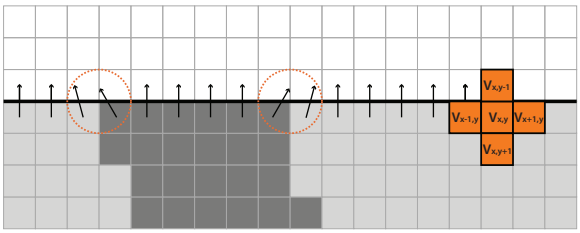

Figure 4: *The dotted circles show the transformed gradients at the tissue boundary for the illumination computation.*

To allow the modification of the bump effect strength we integrate the bump value v_{bump} and evaluate the following equation:

$$i_{sample_j} = (i_{class_j} * v_{bump}) - (v_{bump} - 1)$$

For every sample intensity i_{sample_j} of the on-the-fly computation we weight the intensity of the classified sample i_{class_j} with the bump value v_{bump}. If v_{bump} is near zero, there is no enhancement effect visible. In our examples we used a value of v_{bump} = 1.5. Figure 5 shows that the underlying structures can be better perceived because of the boundary enhancement of the brain structures.

5. Advanced Cutting-Tools for Volume Exploration

Volume data sets are mostly visualized using cutting planes which allow medical experts to explore data sets in three axis aligned directions: in axial direction, in coronal direction and in sagittal direction. Some neurosurgical planning tools provide additional cutting techniques, e.g. cutting in

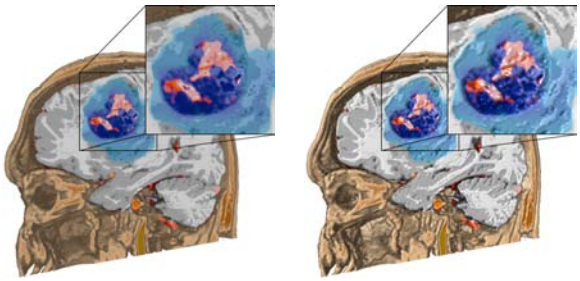

(a) (b)

Figure 5: *In (a) the clipping plane is not illuminated (v_{bump} = 0). Anatomical details in the blue region are difficult to recognize. (b) With enabled boundary enhancement (v_{bump}=1,5), the anatomical structures of the clipping surface can be better distinguished (see also color plate).*

view direction or distance based clipping. The advantage of cutting planes is that anatomical structures can be explored in detail at a specified position of the plane. However, for a complete exploration of the data set substantial interaction is needed. Therefore our goal is to develop novel cutting methods which require minimal interaction and allow an appropriate exploration of the data set.

The idea of the axis aligned cutting tools is based on the traditional exploration of volume data sets in medicine. In the context of volume rendering, the axial cutting plane is used so that the brain is visible from below. But if the angle between view line and cutting plane is too small, the cutting field is not visible anymore and this view becomes unfeasible for exploration. The same problem appears using the sagittal cutting plane. Since the view point can be rotated around the volume rendering, the plane might also cut the false part of the view and would need to be adjusted.

5.1. Automatic Axis aligned Cutting Tool

Our solution to solve this problem is the *Automatic Axis aligned Cutting Tool*. The idea is to discard the part of the volume where the viewpoint is located. A straightforward implementation would be to subdivide the volume into eight octant sectors, with the origin set by the user. Now we could discard those sectors which are located between the origin and the viewpoint. However, with this technique a cutting plane through the whole volume is not possible, since not more than one sector can be located between origin and viewpoint (see Figure 7).

A better solution is to use a sphere with 26 different sectors instead of the eight octants. The 26 different sectors to cut the volume consist of the following cases: six cases for cutting a half (traditional cut plane), 12 cases for cutting a quarter and 8 cases for cutting an eighth. Now we are able to cut more than one octant. If the view point is in one of the

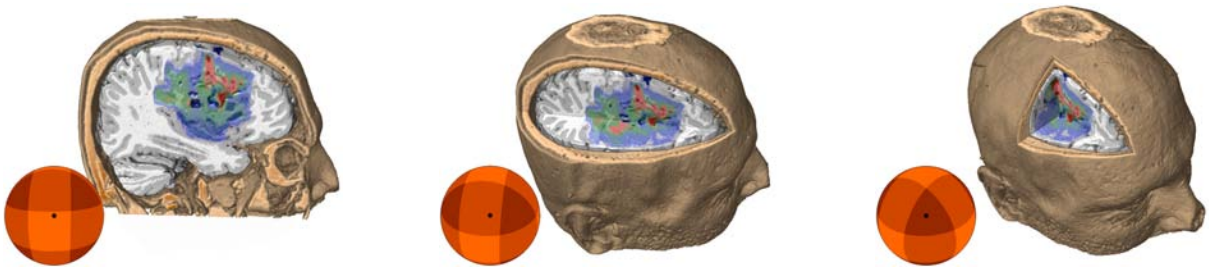

(a) (b) (c)

Figure 6: *Image (a) shows the case that four sectors are hidden, (b) two sectors and (c) a single octant. The black dot in the sphere illustrates in which sector the camera is located.*

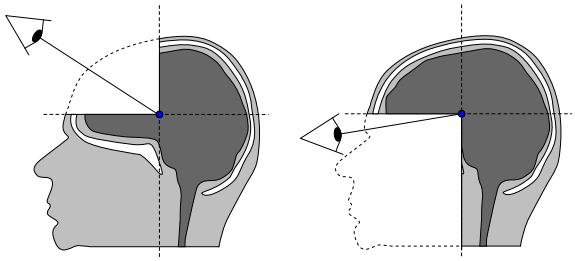

(a) (b)

Figure 7: *This illustration shows four defined sectors in 2D. In (a) the sector which is located between origin and viewpoint is hidden. In image (b), also one sector is hidden but cutting through the whole volume i.e. hiding the sector above, too, is not possible.*

six sectors for cutting a half, the four octants are discarded which occlude the origin. If the view point is in one of the quarters, two octants will be discarded and if in the eighth, one octant will be discarded so that the origin is always visible (see Figure 6). Thus, the manipulation of the cutting area is implicit while rotating the data set and provides a meaningful clipping in consideration of the viewpoint and origin. The only explicit interaction regarding the cutting planes is repositioning the origin, which is required to make important structures visible, that otherwise would be hidden within one of the sectors.

Technically, we use a mask volume for the decision which voxels have to be discarded. This mask volume has the same physical size as the original volume but does not need to have the same voxel size. So we use a very small mask volume with ten times voxel size and a tenth image resolution. In a GLSL shader, the mask volume is moved onto the octants to be hidden. All voxels whose mask value is zero will be discarded. Due to the small mask volume used and the transformation of the mask volume texture coordinates no additional computation time is measurable.

5.2. Two-stage Rendering Pipeline

The disadvantage of using cutting tools generally is that pathological structures are hidden with the occluded anatomy as well. But often an overview of these important structures is advantageous to be able to recognize their complete size and location. If we force the volume renderer to draw voxels whose intensity in the additional volume is high and surrounding voxels are cut away, the structures from the additional data sets are excluded from cutting. However, we are not able to show these structures in a different visualization style because the rendering parameters can just be changed globally (see Figure 8 (a)).

Our solution is to split the rendering pipeline into two parallel stages. The first stage of the pipeline includes the rendering steps to compute the volume rendering of the anatomical structures, which are not clipped away. The second stage is used to specify rendering parameters (gradient computation, classification, lighting) for the visualization of important structures, which are not cut away though they lie in the clipping area (see Figure 8 (b)). For every voxel the intensity

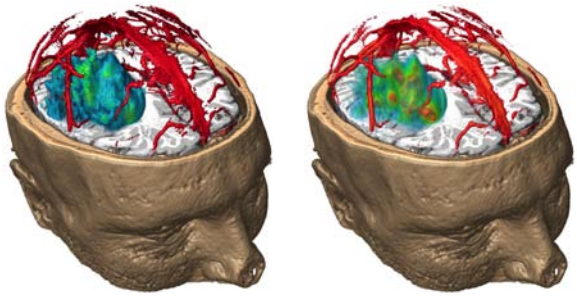

(a) (b)

Figure 8: *In (a) the structures excluded from clipping have the same rendering style. In (b) the rendering style of vessels and pathological structures is changed, so that the internal in-homogeneous structures are visible (see also color plate).*

value of the mask volume is used to decide which rendering stage has to be used for rendering.

5.3. Brain Peeling Cutting Tool

The exploration of anatomical details located in the vicinity of the brain surface is difficult to achieve with cutting planes. For example the examination of vessels located close to the brain surface, so that the complete structure of the vessels is visible, is not possible. Our solution is the *brain peeling cutting tool* which is inspired by opacity peeling [RSK06] and the work of Tappenbeck et al. [TPD06]. *Brain peeling* allows medical experts to peel the brain surface step by step. With this technique the exploration of structures located close to the surface is intuitive to achieve. Figure 9 illustrates that the red lesion just becomes visible if the brain is peeled away from the surface in negative normal direction.

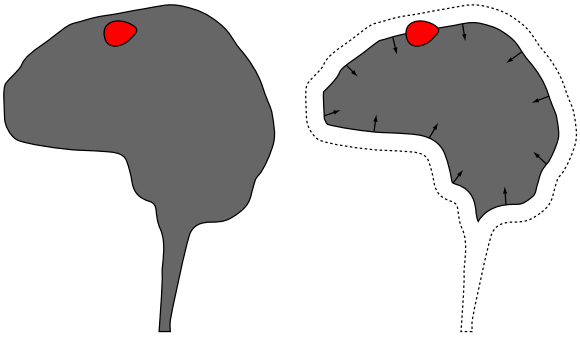

Figure 9: *(a) The tumor, located near the brain surface, is not visible. (b) The brain can be peeled from the surface in negative normal direction so that the tumor can be intuitively explored.*

For the brain peeling algorithm, we compute a distance field using a simple diffusion filter or distance transformation from the extracted brain mask. In a GLSL shader, this volume data set is used to specify the distance to the brain surface for every voxel. If the intensity of the mask voxel is lower than the threshold which encodes the distance, the voxel of the data set will be discarded. The user is able to peel the brain using this single distance threshold. Since robust skull stripping methods like [HP00] exist, our combined approach represents an alternative to opacity peeling. In contrast to opacity peeling, this technique is view independent and depends on less parameters, thus making it more reliable. To get smooth visualization results we blend the alpha values in a small range in normal direction. In Figure 10 (a) some vessel structures are hidden by the brain tissue. If the brain is peeled away (b), the structure of the vessels can be recognized. Also, suspicious high intensity values from T_2-*weighted* or *FLAIR* data sets are visible.

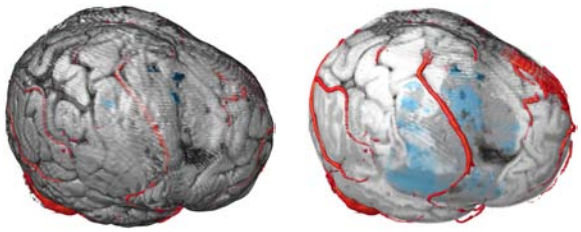

Figure 10: *(a) Structures located near the brain surface are not visible. (b) Using brain peeling, structures like the vessel at the right side are visible.*

6. Results

For a concluding discussion we compared the performance of our rendering techniques. The viewport was of size 512x512, the registered data sets were of size 205x225x158 and the mask used for the automatic clipping tool was of size 21x23x16. To approximate the mean frame rates we rotated the volume rendering by 360 degree in 360 steps. Figure 11 illustrates the resulting frame rates on a Mac Pro 2.66 GHz with 4 GB RAM and an ATI Radeon X1900 graphics card. The highest performance was achieved without clipping computation. On-the-fly gradient computation was always enabled. The rendering of the two additional data sets (T_1ce, *FLAIR*) reduced the performance to 12 fps because of the supplemental texture lookups. The manual clipping technique reduced the performance once more to 8 fps. The loss of performance is due to the additional texture lookups for boundary enhancement. Particularly the automatic cutting tool and brain peeling are beneficial techniques for exploration because of the minimal performance loss compared with manual clipping. In addition, considering that the methods highly depend on the performance of the graphics card a raise in the frame rates can be expected if using a more high-end graphics card.

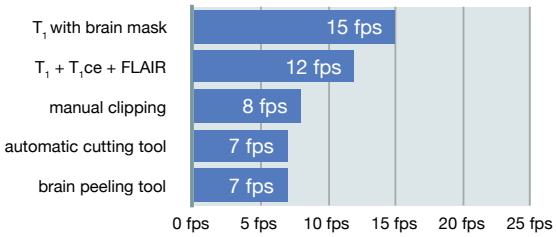

Figure 11: *The additional data sets reduce the performance from 15 to 12 fps. Automatic clipping as well as brain peeling reduces the performance negligible compared with manual clipping.*

7. Discussion and Conclusion

In this paper we described visualization techniques for combining medical multi-spectral MRI data sets. Furthermore, we introduced recent cutting methods for the exploration of anatomical structures combined with inhomogeneous pathological tissue as well as perifocal edema. Our techniques were tested with five clinical data sets and the results were discussed with medical experts who judged the volume visualization methods to provide clear and helpful information for the evaluation of intracerebral spatial relations. We outlined possible automated preprocessing steps focusing on registration, segmentation and histogram data analysis. After fuzzy clustering as a preprocessing step for histogram analysis, we are able to automatically specify transfer functions for blending suspicious intensity values of the additional data set, e.g. FLAIR, as well as contrast enhanced data with the anatomical rendering. These transfer functions can but do not need to be manipulated subsequently by the user. To allow recognition of anatomical details in blended areas we implemented boundary enhancement on clipping planes. To avoid substantial need of interaction in volume exploration, we introduced the automatic cutting tool as well as the brain peeling technique. The medical experts explained that the automatic cutting tool combined with boundary enhancement allows them to intuitively explore the expansive effect of lesions as well as the brain shift caused by large tumors. Furthermore, brain peeling enables the exploration of interesting structures in the vicinity of the brain surface without the need of complicated adjustment of clipping planes. This technique was perceived as very helpful to relate pathological structures to respective vessels.

We are aware that the combination and automatic preprocessing of multimodal MRI data sets presumably leads to inaccuracies as stated by Weiler et al. [WHK*08]. This is an issue that has to be considered especially for the routine application, but since the focus of this work lies on the visualization techniques, the presented preprocessing steps have to be seen as a first approach that has yet to be improved and evaluated in detail.

As future work a comprehensive case study has to be performed to evaluate the clinical value and suitability of the presented combination of methods especially due to the applied heuristics. Furthermore the applicability of the visualization methods for the clinical routine as well as the robustness of the preprocessing should be examined in more detail.

To conclude, our techniques have potential to improve the assessment of spatial heterogeneity of brain tumors, the preoperative planning and risk analysis, and the characterization of pathological changes over time.

References

[BBM*07] BLAAS J., BOTHA C. P., MAJOIE C., NEDERVEEN A., VOS F. M., POST F. H.: Interactive Visualization of Fused fMRI and DTI for Planning Brain Tumor Resections. In *Proc. SPIE Medical Imaging* (2007), vol. 6509.

[Bez81] BEZDEK J. C.: *Pattern Recognition with Fuzzy Objective Function Algorithms*. Kluwer Academic Publishers, Norwell, MA, USA, 1981.

[BGK06] BRUCKNER S., GRIMM S., KANITSAR A.: Illustrative Context-Preserving Exploration of Volume Data. *IEEE Trans. on Visualization and Computer Graphics 12*, 6 (2006), 1559–1569.

[BHC93] BEZDEK J. C., HALL L. O., CLARKE L. P.: Review of MR image segmentation techniques using pattern recognition. *Medical Physics 20* (July 1993), 1033–1048.

[BHWB07] BEYER J., HADWIGER M., WOLFSBERGER S., BÜHLER K.: High-Quality Multimodal Volume Rendering for Preoperative Planning of Neurosurgical Interventions. *IEEE Trans. Vis. Comput. Graph. 13*, 6 (2007), 1696–1703.

[Bli78] BLINN J. F.: Simulation of wrinkled surfaces. *SIGGRAPH Comput. Graph. 12*, 3 (1978), 286–292.

[HBKS05] HONG H., BAE J., KYE H., SHIN Y.-G.: Hardware-accelerated multimodality volume fusion. In *Proceedings of the SPIE Medical Imaging* (Apr. 2005), vol. 5744, pp. 629–635.

[HKRs*06] HADWIGER M., KNISS J. M., REZK-SALAMA C., WEISKOPF D., ENGEL K.: *Real-time Volume Graphics*. A. K. Peters, Ltd., Natick, MA, USA, 2006.

[HP00] HAHN H. K., PEITGEN H.-O.: The Skull Stripping Problem in MRI Solved by a Single 3D Watershed Transform. In *Proceedings of MICCAI* (London, UK, 2000), Springer-Verlag, pp. 134–143.

[JBB*08] JAINEK W. M., BORN S., BARTZ D., STRASSER W., FISCHER J.: Illustrative Hybrid Visualization and Exploration of Anatomical and Functional Brain Data. *Computer Graphics Forum 27*, 3 (2008), 855–862.

[KSW*04] KNISS J., SCHULZE J. P., WÖSSNER U., WINKLER P., LANG U., HANSEN C. D.: Medical Applications of Multi-field Volume Rendering and VR Techniques. In *Proceedings of the Joint Eurographics-IEEE TCVG Symposium on Visualization* (2004), pp. 249–254.

[KWK*07] KÖHN A., WEILER F., KLEIN J., KONRAD O., HAHN H. K., PEITGEN H.-O.: State-of-the-Art Computer Graphics in Neurosurgical Planning and Risk Assessment. In *Proc. of Eurographics Short Papers and Medical Prize Awards* (2007), pp. 117–120.

[PAG03] PIROGOV Y. A., ANISIMOV N. V., GUBSKI L. V.: 3D visualization of pathological forms from MRI data obtained with simultaneous water and fat signal suppression. In *Proceedings of the SPIE Medical Imaging* (June 2003), vol. 5030, pp. 939–942.

[PMV03] PLUIM J. P. W., MAINTZ J. B. A., VIERGEVER M. A.: Mutual-information-based registration of medical images: a survey. *Medical Imaging, IEEE Transactions on 22*, 8 (2003), 986–1004.

[RRRP08] RIEDER C., RITTER F., RASPE M., PEITGEN H.-O.: Interactive Visualization of Multimodal Volume Data for Neurosurgical Tumor Treatment. *Computer Graphics Forum 27*, 3 (2008), 1055–1062.

[RSK06] REZK-SALAMA C., KOLB A.: Opacity peeling for direct volume rendering. In *Computer Graphics Forum* (2006), vol. 25(3), pp. 597–606.

[SDP08] SCHWIER M., DICKEN V., PEITGEN H.-O.: 3D Visualization of Vascular Structures around Liver Tumors using Fuzzy Clustering. In *Proceedings of CARS* (2008), pp. 403–404.

[SSA*08] SCHULTZ T., SAUBER N., ANWANDER A., THEISEL H., SEIDEL H.-P.: Virtual Klingler Dissection: Putting Fibers into Context. *Computer Graphics Forum 27*, 3 (2008), 1063–1070.

[TPD06] TAPPENBECK A., PREIM B., DICKEN V.: Distance-Based Transfer Function Design: Specification Methods and Applications. In *Simulation und Visualisierung* (2006), pp. 259–274.

[VFSG06] VIOLA I., FEIXAS M., SBERT M., GRÖLLER M. E.: Importance-Driven Focus of Attention. In *IEEE Trans. on Visualization and Computer Graphics* (2006).

[WEE03] WEISKOPF D., ENGEL K., ERTL T.: Interactive Clipping Techniques for Texture-Based Volume Visualization and Volume Shading. *IEEE Trans. on Visualization and Computer Graphics* (2003), 298–312.

[WHK*08] WEILER F., HAHN H. K., KÖHN A., FRIMAN O., KLEIN J., PEITGEN H.-O.: Dealing with Inaccuracies in Multimodal Neurosurgical Planning - A Preliminary Concept. In *Proceedings of CARS* (2008), pp. 77–78.

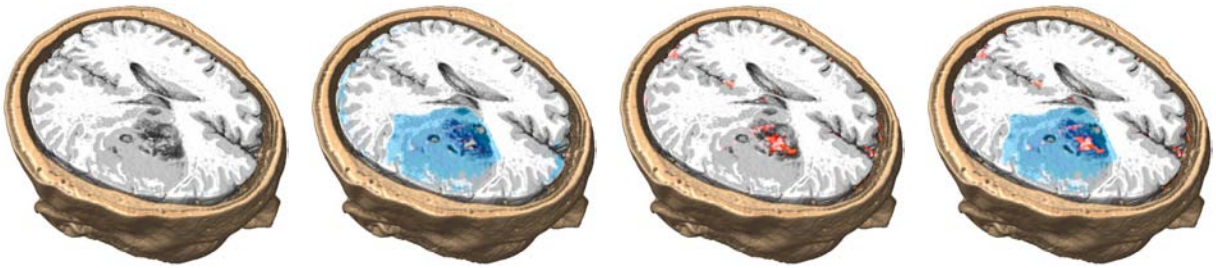

(a) (b) (c) (d)

Figure 3: *Image (a) shows the T_1-weighted data set without blending of additional data sets. In (b) the T_1-weighted data set is blended with the FLAIR data set. The high intensity values are color coded blue and include unimportant structures at the brain boundary. Image (c) shows the color coded structures of the vessel mask and (d) the combination of all data sets, the FLAIR data set is blended using the ROI so that unimportant structures are hidden.*

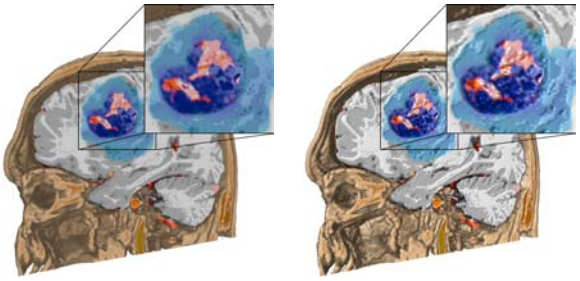

(a) (b)

Figure 5: *In (a) the clipping plane is not illuminated (v_{bump} = 0). Anatomical details in the blue region are difficult to recognize. With enabled boundary enhancement (v_{bump}=1,5), the anatomical structures of the clipping surface can be better distinguished (b).*

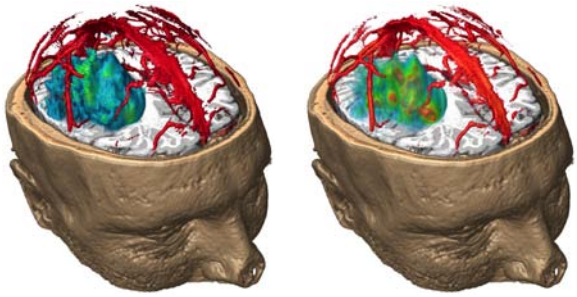

(a) (b)

Figure 8: *In (a) the structures excluded from clipping have the same rendering style. In (b) the rendering style of vessels and pathological structures is changed, so that the internal in-homogeneous structures are visible.*